Journal of Biomedical Optics

BiomedicalOptics.SPIEDigitalLibrary.org

Optical imaging of fluorescent carbon biomarkers using artificial neural networks

Tatiana A. Dolenko
Sergey A. Burikov
Alexey M. Vervald
Igor I. Vlasov
Sergey A. Dolenko
Kirill A. Laptinskiy
Jessica M. Rosenholm
Olga A. Shenderova

SPIE.

Journal of Biomedical Optics 19(11), 117007 (November 2014)

Optical imaging of fluorescent carbon biomarkers using artificial neural networks

Tatiana A. Dolenko,[a,*] Sergey A. Burikov,[a] Alexey M. Vervald,[a] Igor I. Vlasov,[b,c] Sergey A. Dolenko,[d] Kirill A. Laptinskiy,[a] Jessica M. Rosenholm,[e] and Olga A. Shenderova[g]
[a]M. V. Lomonosov Moscow State University, Department of Physics, Leninskie Gory 1/2, Moscow 119991, Russia
[b]A. M. Prokhorov General Physics Institute, RAS, Vavilova Street 38, Moscow 119991, Russia
[c]National Research Nuclear University MEPhI, Kashirskoe Avenue 31, Moscow 115409, Russia
[d]M. V. Lomonosov Moscow State University, D. V. Skobeltsyn Institute of Nuclear Physics, Leninskie Gory 1/2, Moscow 119991, Russia
[e]Abo Akademi University, Laboratory for Physical Chemistry, Porthansgatan 3, 20500 Turku, Finland
[g]Adámas Nanotechnologies, Inc., Raleigh, North Carolina 27617, United States

Abstract. The principle possibility of extraction of fluorescence of nanoparticles in the presence of background autofluorescence of a biological environment using neural network algorithms is demonstrated. It is shown that the methods used allow detection of carbon nanoparticles fluorescence against the background of the autofluorescence of egg white with a sufficiently low concentration detection threshold (not more than 2 μg/ml for carbon dots and 3 μg/ml for nanodiamonds). It was also shown that the use of the input data compression can further improve the accuracy of solving the inverse problem by 1.5 times. [DOI: 10.1117/1.JBO.19.11.117007]

Keywords: carbon nanoparticles; autofluorescence; optical imaging; neural networks.

Paper 140462R received Jul. 18, 2014; revised manuscript received Oct. 4, 2014; accepted for publication Oct. 15, 2014; published online Nov. 14, 2014.

1 Introduction

One of the main focuses of modern biomedicine is the development of supersensitive and high-throughput methods for rapid detection of proteins and genes as well as visualization of biomarkers and drug carriers in biological material.[1–3] The most widespread method of recognition of biomarkers and study of cellular interactions is visualization by means of fluorescence. However, a variety of complications exist in the tracking of fluorescent markers in the biological environment. Most of the fluorescent markers are excited by ultraviolet or visible radiation and emit in the visible spectral range. However, in this spectral range, biological tissue absorbs and emits light strongly.[1–3] Therefore, illumination of the biological material in this range induces fluorescence of the living tissue (autofluorescence), which is caused by natural fluorophores (tryptophan, phenylalanine, tyrosine, collagen, flavins and flavoproteins, beta-carotene, porphyrins, nucleic acids, coenzymes, vitamins, pigments and so on[4]). The spectrum of the autofluorescence is the result of superposition of fluorescence bands of fluorophores, vastly complicating the observation of cellular processes and the tracking of the fluorescent markers.

Currently, there are two major approaches to overcome the problem of background fluorescence:

(1) synthesis of new biomarkers with minimum overlap of their emission spectra with the background fluorescence[2–25] and (2) development of advanced experimental techniques permitting one to decrease the background signal.[26–34]

Intense work is being carried out on the search for and synthesis of nanoparticles with optimal properties for biological applications as biomarkers, absorbents, and drug carriers.[2–5] The existing biomarkers have several drawbacks. Molecules of organic dyes have a high intensity of luminescence per mass unit but they are not suitable for long-term *in vitro* and *in vivo* control because of fast photobleaching and cellular toxicity.[6] Even dyes with improved properties, created, for example, by combinatorial organic synthesis,[7] are not photostable.

In comparison with organic probes, semi-conducting quantum dots have a few major advantages:[8,9] high quantum yield and photostability, broad excitation range, and narrow emission band with the emission maximum strongly depending on the size of the quantum dot. The drawbacks include cytotoxicity, which is still debated, and luminescence blinking.[8,9]

Promising materials for optical imaging are fluorescent carbon nanoparticles such as nanodiamonds (NDs),[10–16] carbon dots/graphene oxides (CD/GO),[17–19] and nanodiamonds decorated with carbon dots (CD-D-ND).[20] Apart from outstanding photostability and high quantum efficiency, CDs and NDs have poly-functional surfaces which can be modified to address specific needs. Methods of coating carbon nanoparticles with polymers or mesoporous silica shells have been developed. These coatings improve biocompatibility and decrease the toxicity of the particles while preserving their fluorescence properties.[21–25] A drawback of the carbon nanoparticles is a broad emission band overlapping with the autofluorescence, which does not provide the required contrast in particles imaging.

Thus, despite significant progress in the synthesis of new nanoparticles for biological applications, a big challenge remains in the development of nontoxic imaging probes providing a highly reliable visualization in combination with a pronounced therapeutic effect.

Most of the methods of optical imaging are based on optical microscopy.[26–30] Confocal laser scanning microscopy (CLSM)

*Address all correspondence to: Tatiana A. Dolenko, E-mail: tdolenko@lid.phys.msu.ru or tdolenko@mail.ru

0091-3286/2014/$25.00 © 2014 SPIE

is a commonly used tool that provides morphological and functional information within cells and tissues.[28,29] It was shown that the unique capabilities of CLSM such as the ability to detect fluorescence, three-dimensional (3-D) image reconstruction, and use of the reflection mode in tandem with other methods, provide great promise with broad applications for the visualization of various nanoparticles such as quantum dots, fullerenes, dendrimers, for example, at their penetration into the surface of the skin. It was shown that multiphoton excitation microscopy has advantages over conventional one-photon imaging microscopy and can be used as a modern noncontact tool for 3-D fluorescence imaging and optical diagnostics.[31,32]

For visualization of markers within tissue, the capability of metal nanoparticles to generate plasmons while interacting with an electromagnetic field is widely used.[33,34] Thus, a dark-field microspectroscopy technique for molecular imaging of live cells using antibody-labeled plasmonic nanoparticles was demonstrated.[33,34] Experiments have shown that the accuracy of the visualization is influenced both by interactions of the nanoparticles with biomacromolecules and by the interactions of interparticle plasmons.

Rapidly developing methods of visualization of nanoparticles in biological tissues include photoacoustic high-resolution imaging[35,36] and high-sensitivity real-time radiometric imaging of nanoparticles with surface-enhanced Raman scattering.[37,38]

One of the approaches to solve the problem of autofluorescence suppression is the synthesis of new nanoparticles called upconversion nanoparticles (UCNPs).[39–41] These particles have improved luminescence properties (the emission/excitation power ratio[39]). UCNPs properties allow strong suppression of background signals (excitation light back-scattering and biological tissue autofluorescence). Currently, UCNPs particles are among the most promising for bionanomedicine.

Together with the microscopy technical capabilities, methods of image processing are also being developed. Recent progress in the 3-D single particle tracking is summarized in the review by Dupont and Lamb.[42] A modified version of the original orbital tracking in which the intensities from two z-planes are simultaneously measured is demonstrated. The precision of single particle tracking is ~5 nm in the x-y plane and ~7 nm in the axial direction.

Now, methods of background-free fluorescence based on fluorescence modulation by electromagnetic or magnetic fields combined with image subtraction are actively being developed. Igarashi et al.[43] improved the image contrast of fluorescent NDs (FNDs) *in vitro* as well as *in vivo* based on the spin property of the NV– center. The authors acquired wide-field fluorescence images with and without microwave irradiation in resonance with the crystal-field splitting (2.87 GHz) of the ground-state spin, and then performed subtraction between these two images pixel by pixel. As the alternative microwave irradiation modulated only the fluorescence intensity of the NV– center, the operation effectively removed background autofluorescence signals and significantly improved the image contrast. Similarly, Hegyi and Yablonovitch[44] applied the optically detected magnetic resonance technique to image FNDs in tissue in the field-free region using an amplitude-modulated microwave source. More recently, Sarkar et al.[45] utlized a modulated external magnetic field to achieve contrast enhancement of FNDs *in vivo*. The magnetic field mixes the spin levels at the ground state, resulting in modulation of the FND fluorescence. As a demonstration of the potential translational relevance of the work, where unique improvements to imaging efficiency were observed, this technique improved the image contrast by nearly two orders of magnitude, allowing for wide-field imaging of FNDs in sentinel lymph nodes of mice.

Thus, the problem of optical imaging of nanoparticles or cells in biological tissues is currently being solved by synthesis of novel nanoparticles or nanocomposites and their optimization and through improvement of advanced equipment and methods of image processing. At the same time, in all the methods under development, there remains a problem of accounting for interactions between nanoparticles and biomaterial, requiring intensive study.

In this paper, a new approach to solve the inverse problem of separation of the fluorescent signal of nanoparticles from the background autofluorescence is proposed based on artificial neural networks (ANNs).[46] ANNs represent powerful data analysis algorithms which provide an efficient solution of inverse problems and problems of pattern recognition, including those in optical spectroscopy.[46–50] Artificial intelligence techniques are practically used in all fields of bioinformatics,[47] since there are no universal methods of data processing comparable to the efficiency of human intellectual potential. It is very promising now to use ANN for the solution of such problems as a method for classification of proteins, selection of genome fragments, recognition of signal peptides and transmembrane helices, and so on.[51] In Refs. 52 and 53, the method of breast cancer diagnosis based on ANN classification was proposed. The inverse problem of autofluorescence recognition of cell culture and cancer cells was solved. Total synchronous fluorescence spectra of normal skin, nevus, and melanoma samples were used as input for training the ANNs. Two different types of ANNs were trained, the self-organizing map and the feed-forward neural network. Histopathology results of investigated skin samples were used as the important standard for network output. Based on the obtained classification success rate of neural networks, Dramićanin et al.[52] concluded that both networks provided high sensitivity with classification errors between 2% and 4%. Despite the extremely wide application of pattern recognition methods in biomedicine, to the authors' knowledge, this paper is the first application of these methods for detection of the fluorescence of nanoparticles in the presence of background autofluorescence.

In the current paper, the method was elaborated for selected fluorescence nanoparticles—CDs[17] and nanodiamonds and using a particular biological object—chicken egg white. Proof of concept of fluorescence biomarkers visualization in biological media using neural network algorithms was demonstrated. The minimum concentration of nanoparticles that can be reliably detected in the presence of autofluorescence background using ANN was determined. Ways to improve the sensitivity of the ANN method at solving the above inverse problem are also discussed.

2 Experimental

2.1 *Carbon Nanoparticles and Their Characterization*

In this study, nano-graphene oxide (NGO) particles[17] and detonation nanodiamond G01 (PlasmaChem, Germany) were used. NGO nanoparticles were synthesized by oxidizing nanographite in a 3:1 sulfuric to nitric acids mixture at a temperature of 130°C. The reaction supernatant was collected by removing the

graphitic carbon residue by centrifugation. The supernatant was neutralized by the addition of sodium hydroxide. The neutralized solution was dialyzed for 2 days against water.[17] Below, they are called CD.

Nanodiamonds G01 were prepared by controlled dry detonation synthesis followed by purification. The bulk powder density of the sample was 0.69 g/cm^3, the primary particle size was about 4 nm.

Bidistilled deionized water was used for the preparation of aqueous suspensions of carbon nanoparticles. Aqueous suspensions of CD with a concentration of 0.1 g/l and aqueous suspension of ND with a concentration of 1 g/l were prepared. Suspensions were treated for 2 h in an ultrasonic bath (Bandelin Sonorex rk 31).

Measurements of the sizes of CD and ND in water suspensions were carried out by the method of dynamic light scattering using correlator-goniometer system ALV-CGS-5000/6010 (Langen, Germany), equipped with a He-Ne laser (at a wavelength of 633 nm, output power 20 mW). For numerical processing of the correlation functions, the software package CONTIN was used. Measurements showed that the majority of the CD particles in water had dimensions of $6-9$ nm, and 88% of the ND particles in the suspension had a size of 35 nm.

2.2 *Biological Media*

As a biological media, chicken egg white was chosen. This choice is justified by the fact that delivery of nanoparticles directly into the cell is provided, as the whole egg white is a single cell. Also the choice is associated with representative natural fluorophores in the egg white.

In subsequent experiments, in order to improve the reliability of the trained neural network toward changes in biological objects, egg whites of different stages of development and from different vendors were used.

2.3 *Quantum Efficiency and Photostability of Carbon Nanoparticles*

For the use of fluorescence nanoparticles in biological applications, high quantum yield, photostability and low toxicity are required.

2.3.1 *Quantum yield of fluorescence of carbon nanoparticles*

The fluorescence quantum yield is a critical parameter in selecting a material as a biomarker.

In this paper, the fluorescence quantum yields of CD and ND were measured by a standard method relative to a reference dye quinine sulfate. The absorption spectra of the aqueous suspensions of CD and ND were recorded by spectrophotometer Perkin Elmer Lambda 25 in the range 200 to 900 nm with a resolution of 0.5 nm. Spectra of fluorescence of suspensions were recorded by fluorimeter FluoroMax-4 (Horiba Jobin Yvon). The obtained fluorescence spectra were corrected for absorption. The measured values of the quantum yields of CD and ND are 3.07% (at a wavelength of 405 nm) and 0.47%, respectively.

Previously, neural network algorithms were tested by us to separate the fluorescence signal of the CD from background autofluorescence.[54] In this paper, it is shown that ANN provides much greater sensitivity of detection of the fluorescent signal: using neural network algorithms, a method of recognition of fluorescent nanoparticles with a much lower quantum efficiency was elaborated (the quantum yield of detonation nanodiamonds is 6.5 times lower than the quantum yield of CD).

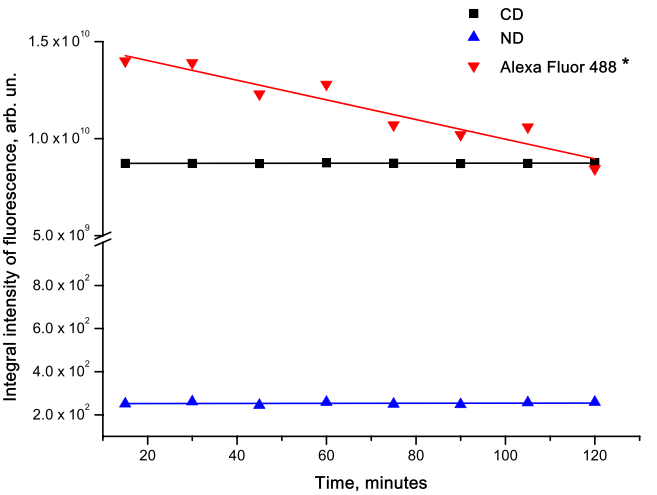

Fig. 1 Dependence of the integral fluorescence intensity of carbon dots (CDs), nanodiamonds (NDs) and dye Alexa Fluor 488 as a function of time of the laser irradiation of the suspensions.

2.3.2 *Photostability of aqueous suspensions of carbon particles*

We carried out a comparative analysis of the temporal stability of the fluorescence of water suspensions of CDs, the typical detonation ND, and organic dye Alexa Fluor 488 with the same concentration, 0.3 g/l.

A cuvette with a suspension of nanoparticles was fixed in the cell holder and constantly exposed to laser radiation (argon laser, at a wavelength of 488 nm, power density in cuvette about 10 W/cm^2 in a defocused beam) for 2 h. Spectra were measured every 15 min in the spectral range 500 to 800 nm using a photomultiplier tube (PMT) (Hamamatsu, H-8259-01) in photon counting mode. The geometry of the experiment and the experimental conditions were exactly the same for all samples. Spectra were corrected for laser power, data acquisition time, sensitivity of the PMT, and absorption of samples.

Figure 1 shows the dependence of the integral intensity of the fluorescence of the studied suspensions as a function of irradiation time. The experimental results clearly demonstrate the advantages of photostability of carbon nanoparticles as compared with the organic dye.

3 Fluorescence Spectroscopy of Biological Objects with Carbon Nanoparticles Ion

3.1 *Laser Spectrometer*

Fluorescence and Raman signals from aqueous suspensions of nanoparticles and biological objects containing nanoparticles were excited by a diode laser (at a wavelength of 405 nm, power incident on the sample ~50 mW). Spectra were recorded by PMT (Hamamatsu, H-8259-01) in the range 430 to 750 nm. The practical spectral resolution was 0.5 nm. The temperature of the samples was stabilized at 22.0 ± 0.1°C. Spectra were corrected for the laser power and data acquisition time. Further, mathematical data processing consisted of the subtraction of the background caused by light scattering in the cuvette with the sample and

normalization of the obtained spectra by the area under the Raman valence band of water.

3.2 *Analysis of the Fluorescence Spectra of Egg White with Introduced Carbon Nanoparticles*

Figures 2 and 3 show Raman and fluorescence spectra of egg white, water suspensions of CD and ND, and egg white with introduced nanoparticles. The relatively narrow band near 470 nm is the Raman valence band of OH-groups either of water or of biological media (percentage of water in the egg white is about 85%) under excitation at a wavelength of 405 nm. This band is caused by the valence vibrations of molecular OH-groups (wavenumber of this band maximum is 3400 cm^{-1} and width is about 400 cm^{-1}).

The spectrum of autofluorescence of egg white in the studied range consists of several bands: an intense broad structureless band in the range 430 to 730 nm with a maximum at 480 nm, and weaker bands with maxima at 640 nm, 655 to 660 and 675 nm. It is known[4] that the basic fluorescence band of egg white is formed by the fluorescence contributions of pyridoxine, NADF, flavins, and lipo pigments. Weak fluorescence bands near 640 to 670 nm are caused by the fluorescence of porphyrins.

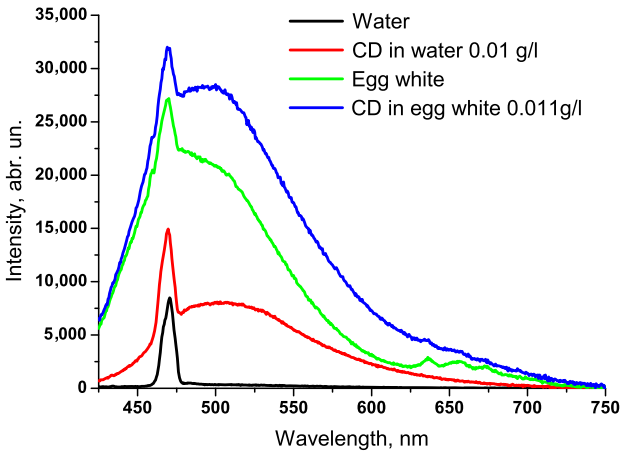

Fig. 2 Raman and fluorescence spectra of water, egg white, aqueous suspensions of CD and egg white containing CD.

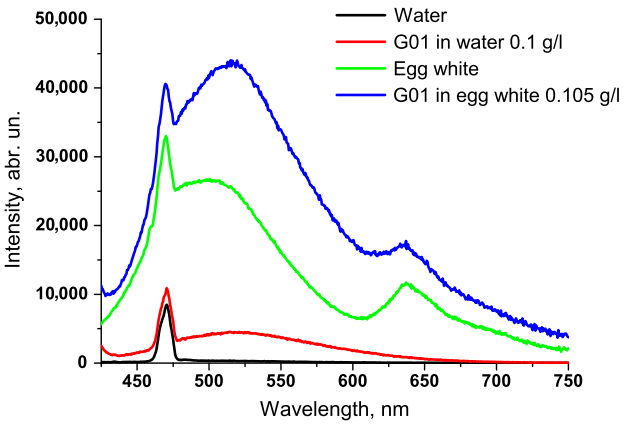

Fig. 3 Raman and fluorescence spectra of water, egg white, aqueous suspensions of ND and egg white containing the ND.

As seen from Figs. 2 and 3, when excited at a wavelength of 405 nm, CDs exhibited fluorescence in the spectral region between 430 and 680 nm with a maximum near 500 to 505 nm, while NDs emit in the region 430 to 680 nm with a maximum near 520 to 525 nm. Egg white emits in the region 420 to 700 nm with a maximum which varies for different eggs within 480 to 520 nm (see below). Thus, the fluorescence spectra of nanoparticles and egg white are largely overlapping structureless bands. They differ in the position of the maximum and the position and extent of the fluorescence spectral bands. These characteristics are the basis for the extraction of the fluorescent signal of the nanocarbon particles.

Obviously, if the concentration of nanoparticles in the egg white changes, the band of the integral fluorescence varies significantly for several reasons. The main reasons are as follows: (1) when the concentration of nanoparticles changes, the intensity of the fluorescence of individual particles changes and (2) due to the interactions of CD and ND with components of the egg white, both the fluorescence of the egg white and that of nanoparticles change. These interactions are very complex and still not well understood in part because the carbon nanoparticles have been relatively recently synthesized. Using conventional methods, it is impossible to construct a mathematical model of the change of the overall fluorescence of an egg white and nanoparticles as a function of their concentrations (for example, during movement of nanoparticles in biotissue). This means that traditional mathematical methods cannot solve either the direct problem of spectra modeling, or the inverse problem of extracting the fluorescent contribution of varying amount of nanoparticles against a background fluorescence of egg white. Therefore, the algorithms of ANNs have been used.

4 Artificial Neural Networks

4.1 *Multilayer Perceptron*

In this study, we use the most widespread type of ANNs such as the multilayer perceptron (MLP). The elementary unit used to construct a MLP is a so-called formal neuron, a unit with several inputs and a single output. Each of the inputs is characterized by its own weight coefficient, w_j. The value y at the output of a neuron is calculated as a weighted sum of the values x_j at its inputs, put through a nonlinear function F called activation function:

$$y = F\left(\sum_{j=0}^{N} w_j x_j\right), \qquad x_0 \equiv 1. \tag{1}$$

Now, identical neurons, different only by their weights, are combined into blocks, which are used to create layers. Each neuron is connected with each of the neurons in the preceding and the next layers (fully connected scheme) (Fig. 4). The signal is fed, according to Eq. (1), from the input of the first layer of the MLP to the output of the last one.

The first layer of an MLP is called the input layer, as it is used to feed data into the MLP, and serves as the input for the whole network. There are as many neurons in the input layer as there are features describing each of the processed data samples. The neurons of the input layer perform no calculations; they simply distribute the input signal to all the neurons of the next layer.

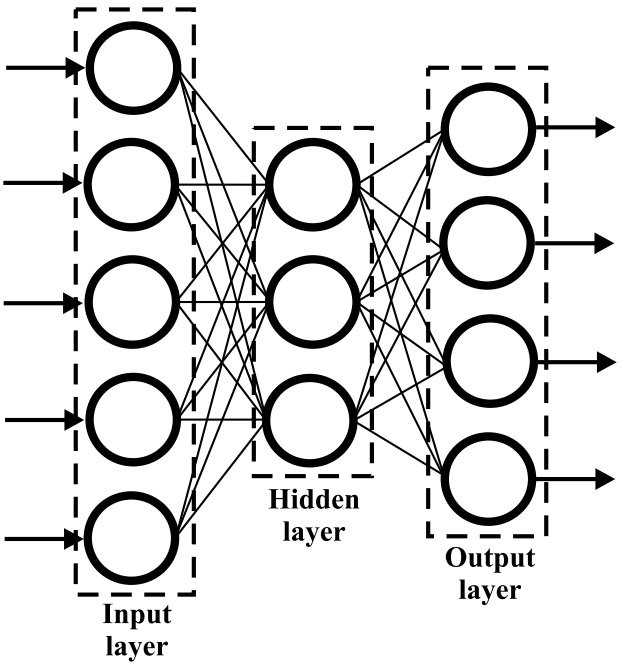

Fig. 4 Multilayer perceptron.

The last layer of an MLP is called the output layer; it serves as the output of the whole network. There are as many neurons in the output layer as there are values that are to be simultaneously determined for each data sample. One or several layers between the input and the output layers are called hidden layers. The numbers of neurons in the hidden layer(s) determine the complexity of the network; it can be estimated by some half-empirical equations, but often it is determined by trial and error.

When the MLP is applied, its output depends on the values of the weight coefficients w (1). Hence, to provide correct answers for an MLP, it should be trained prior to its application. This is done by analyzing the answers of the MLP on the samples of the training set of data, for which the correct (desired) answers are known, with subsequent tuning of the weight coefficients. The goal of training is to minimize the average error of the MLP over the training set by changing the values of the weight coefficients of all the neurons. Most often this is performed by the so-called error backpropagation algorithm, which performs gradient descent in the space of weight coefficients.[46]

4.2 *Use of Artificial Neural Networks to Solve Inverse Problems*

Application of ANN for solving inverse problems of optical spectroscopy is possible using three approaches: "model," "quasi-model," and "experiment-based."[48]

In the "model" approach to obtain a learning sample for ANN training, one applies an existing analytical or computational model of the solution of the direct problem. In the presence of such a model, it is possible to provide the required representativity of all the datasets necessary for ANN training (description of the necessary datasets into which the total learning sample should be divided is provided in Sec. 5.3). However, the quality of solution in this case depends on the adequacy of the model used. In situations where the development of an adequate model is impossible because of the complexity of the object, this approach is not feasible.

In the "quasimodel" approach, in order to obtain representative datasets, simulated spectra are used. Unlike the "model" approach in which the data for the learning sample are calculated according to the known analytical expression describing the spectra, in the "quasimodel" approach, first a parametric "quasimodel" describing the spectra on the basis of a small set of experimental data is constructed, and then it is used to compute the data for the learning sample. Obviously, in this way, a sufficient number of patterns can be obtained providing a good representativity of all sets for ANN training. However, the accuracy of solving the inverse problem with the "quasimodel" approach largely depends on two factors: (1) the error of the "quasimodel" used for the calculation (i.e., correspondence of the selected or calculated "quasimodel" with reality) and (2) differences of the noise in calculated patterns and the noise in real experimental data.

In the "experiment-based" approach, experimental data are used to train the neural network. The disadvantage of this approach is the low representativity of sets because getting a very large amount of experimental material is very time consuming. The main advantages of this approach include: training neural network directly on the experimental data taking all molecular interactions into account, and the fact that the network is trained on real experimental noise, which increases the accuracy of the solution of inverse problems.

As was mentioned above, a problem of recognition of the nanoparticles' fluorescence in the presence of the background fluorescence of egg white cannot be solved based on the "model" approach due to the lack of a correct analytical description of the fluorescence spectra of nanoparticles and the egg white. In addition, because the object of the study is a living biological material and its state can vary significantly with time, it is especially important to train the ANN on real signals of objects containing noise. Thus, in this paper, the inverse problem was solved by ANN in the framework of the "experiment-based" approach.

5 Results and Discussions

5.1 *Experimental Learning Sample for Artificial Neural Networks*

Two series of Raman and fluorescence spectra were obtained for two different egg whites containing CD. The CD concentration varied in the range from 0 to 20 μg/ml with increments of 0.75 and 1.5 μg/ml. Three series of three egg whites containing ND were obtained. The concentration of ND varied from 0 to 30 μg/ml with increments of 1, 1.5, and 3 μg/ml.

To improve the stability of the solution relative to the biological object model, different series of spectra were recorded with different egg whites. As seen from Fig. 5, such an approach is justified since the fluorescence spectra of different egg whites are significantly different. At that position and shape of integral fluorescence band of pyridoxine, NADF, flavins, lipo pigments (430 to 730 nm), and band of porphyrins (640 to 670 nm) remain practically unchanged.

Figure 6 shows examples of the experimental Raman and fluorescence spectra of egg whites with different concentrations of nanoparticles. As seen from Fig. 6, the water Raman valence band (in the region 470 nm) and fluorescence bands of porphyrins (bands near 640 to 670 nm) practically do not change while the fluorescence contribution of CD in the integral fluorescence

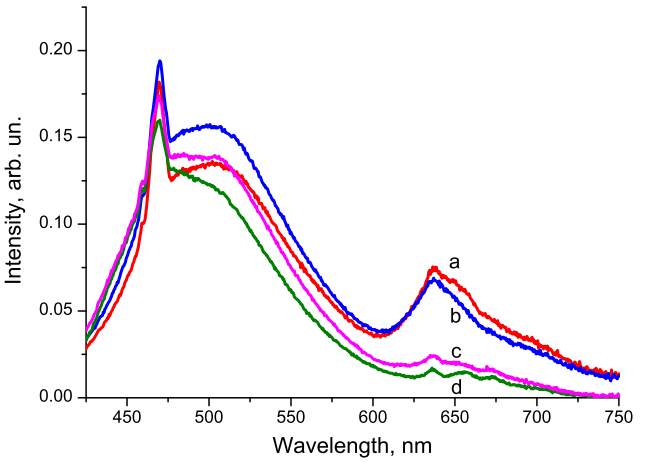

Fig. 5 Fluorescence spectra for different egg whites: a, b, c—egg whites from different vendors; d—egg white after 3 weeks.

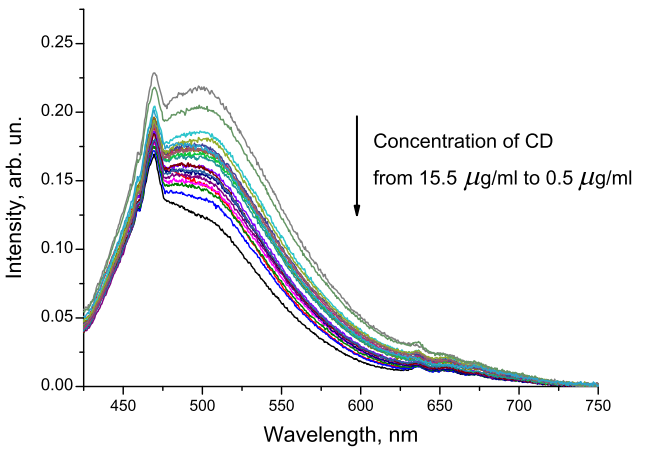

Fig. 6 One of the series of Raman and fluorescence spectra of egg whites with different concentrations of introduced carbon dots.

band in the region 430 to 600 nm changes. The obtained datasets for CD and ND were used for the training of ANN.

5.2 *Preliminary Processing of Input Data*

The considered problem in its original formulation is characterized by an extremely unfavorable ratio of the number of patterns in the training set (30 to 45) and the number of input features (651 points–wavelengths of spectra). Therefore, an important area of research is the use of algorithms to reduce the input dimensionality of the problem, i.e., to reduce the number of input features.

Previous studies made by the authors of this work[55] showed that one of the most effective ways to reduce the dimensionality of the spectroscopic data is the aggregation of the channels of a spectrum. Newly generated features represent the sum of the intensities in several adjacent channels of the spectrum. Apart from the possibility of improving the quality of the problem solutions, this approach, if successful, may allow the use of much less expensive equipment with a significantly lower spectral resolution.

In this paper, two methods have been explored in order to decrease the dimensionality of the input data: channel aggregation, and selection of the most significant features based on the standard deviation of the values in a channel, proportional to the amount of information contained in that channel.

These studies are important not only from the viewpoint of increasing the sensitivity of the method, but also from a practical point of view. Thus, the aggregation of every four channels corresponds to a coarsening of the spectral resolution of the registration devices by four times (from 0.5 to 2 nm). The spectral range of registration is usually chosen in a way to include the entire bands of interesting objects. Discarding insignificant input features allows one to select the most informative region of the spectra and to use the device with registration in the more narrow spectral range.

5.3 *Results of Using Artificial Neural Networks*

For the correct realization of the "experiment-based" approach to ANN training, the learning sample containing the experimental data must be divided into three datasets: training, test, and examination. The training set is used for actual ANN training; the test set—for periodic testing of the network during the learning process in order to determine the moment of termination of the training and to prevent network overtraining; the examination set—to check the quality of the network on an independent dataset. In this paper, this partitioning was carried out randomly in the ratio of 70:20:10 (training-test-examination). As a result, for the spectra of egg white containing CD, the partitioning of 31:8:4 (total 43 patterns) was obtained, and for the spectra of egg white with ND–45:12:6 (total 63). For an unbiased evaluation of the quality of the networks, averaging over 10 random partitionings was conducted for each type of dimensionality reduction of the input data.

To solve this problem, we used a three-layer perceptron (with 10 neurons in the single hidden layer), trained by the error backpropagation algorithm[46] with the following parameters: the hyperbolic tangent transfer function in the hidden and output layers, learning rate 0.01, moment 0.5, the initial dispersion of weights 0.3, random order of presentation of patterns, and stop after 100,000 training events after the minimum of the average error on the test dataset. The software package NeuroShell 2[56] was used for all calculations.

Tables 1 and 2 show the best results of ANN applied to examination sets for different experimental series, for various partitionings into training, test, and examination sets, and after averaging over 10 partitionings, for the original dataset and after the use of the methods of dimensionality reduction for the space of input features. As seen, the error on the examination set for the initial array of data for CD is on the average 2.2 μg/ml, and for ND–4 μg/ml. The high value of the coefficient of multiple determination R^2 should be noted. It indicates effective ANN training.

As seen from these results, both methods used to reduce the dimensionality of input feature space decrease the error. In the case of aggregation, significant features are concentrated in a smaller number of channels without loss of representativity. In the case of discarding insignificant features, the same principle operates: the network is trained better when more information is concentrated in fewer input features without loss of representativity. Table 1 shows the best results, which were obtained by aggregation over four channels. However, the removal of uninformative channels turned out to be more effective. As a result, the average error on the examination set decreased by one and a half times.

The obtained results show that, on average, the error of determination of the concentration of nanoparticles in the studied

Table 1 Results for average error on examination set for the best partitioning.

	Type of preprocessing	Number of features	R^2 on the training set	Average absolute error on the examination set, μg/ml
CD, 43 patterns;	No preprocessing	651	0.9993	1.61
Partitionings	Aggregation	163	0.9833	1.14
31:8:4	Selection	346	0.9525	0.70
ND, 63 patterns;	No preprocessing	651	0.9948	2.41
Partitionings	Aggregation	165	0.9954	1.04
45:12:6	Selection	330	0.9954	0.91

Table 2 Results of averaging over 10 different partitionings: mean ± standard deviation.

	Type of preprocessing	Number of features	R^2 on all patterns	Average absolute error on the examination set, μg/ml
CD, 43 patterns;	No preprocessing	651	0.918 ± 0.021	2.2 ± 0.4
Partitionings	Aggregation	163	0.935 ± 0.036	1.9 ± 0.5
31:8:4	Selection	346	0.925 ± 0.027	1.4 ± 0.4
ND, 63 patterns;	No preprocessing	651	0.837 ± 0.106	4.0 ± 2.0
Partitionings	Aggregation	165	0.832 ± 0.112	3.5 ± 1.6
45:12:6	Selection	330	0.910 ± 0.084	2.5 ± 1.0

volume on the examination set for CD is half as much as for ND. It was expected since, first, the quantum yield of CD for the used excitation wavelength (405 nm) is approximately 6.5 times higher than the quantum yield of ND. Second, the size of ND is several times larger than the size of CD, which causes more intense scattering of light by nanoparticles, and this, in turn, can introduce an additional error in the registration of the spectra.

Thus, the results of the use of ANN showed the principle possibility of solving the problem of separation of the fluorescent contribution of carbon nanoparticles from the background autofluorescence. After reducing the dimensionality of the input data feature space, the attained accuracy of determination of the concentration (on examination set) in the studied volume is up to 2 μg/ml for CD and 3 μg/ml for ND, which is also equal to the minimum detectable concentration of nanoparticles.

5.4 *Prospects of the Proposed Method*

In this study, the successful detection of fluorescent nanoparticles in biological objects using ANN was demonstrated. The presented method is fast, sensitive, inexpensive, and nondestructive. Obviously, in this case it is possible to operate with blood, skin, subsurface vessels, lymph nodes, excretas, and cells *in vivo* and *in vitro*. In our study, the suggested method was elaborated for fluorescent nanodiamond particles and CDs. However, this method can be also used to work with other fluorescent nanoparticles having fluorescence spectra different from the fluorescence spectra of natural biofluorophores, even to a small degree. Note that the suggested method of using ANN is very sensitive. It may provide good optical visualization not only for nanoparticles having a strong fluorescence as a result of some pretreatment (e.g., nanodiamonds after creation of vacancies by electron bombardment or surface modification), but also for nanoparticles with less intense fluorescent properties (detonation nanodiamonds). In this paper, this can be seen from the comparison of the results of ANN application for CD and detonation ND.

As the elaborated method not only provides optical visualization of nanoparticles in biological tissue, but also allows an estimation of their concentration, it can be used for monitoring the distribution of nanoparticles in biomaterial and of their excretion from the organism. This is especially important when nanoparticles (e.g., nanodiamonds or nanocomposites based on nanodiamonds) are used not only as fluorescent biomarkers, but also as drug carriers.[10,12,15,20,22,24] ANNs allow not only the detection of the fluorescent signal of nanoparticles carrying drugs or without drugs against the background of autofluorescence, but also the distinguishing of fluorescence spectra of nanoparticles in both states. This means that the suggested method is capable of providing all the necessary stages of a biomarker "job": monitoring of address delivery, of drug release degree, and of excretion of nanoparticles from the organism.

It should be noted that for each type of biomaterial and nanoparticles, it is necessary to obtain a new experimental database and to retrain the ANN. However, such retraining is performed only once, whereupon the trained ANN can be repeatedly used to solve this specific problem, providing express solution of this problem in real-time experiments.

Unfortunately, so far it is impossible to obtain a fluorescence signal from the deeper layers of the biological system. However, the elaborated method can be also used for detection of signals from deeper layers of bio-objects (for example, when x-ray sources of excitation are used).

6 Conclusion

In this paper, the principle possibility of solving the inverse problem of optical imaging – extraction of the fluorescence of nanoparticles in the presence of background autofluorescence of the biological environment using neural network algorithms was demonstrated. It is shown that the used methods allow detection of CD and ND fluorescence against a background of the autofluorescence of egg white with a sufficiently low concentration for the detecting threshold (not more than 2 μg/ml for CD and 3 μg/ml for ND). It was also shown that the use of the input data compression by aggregation or selection of initial spectral channels can further improve the accuracy of solving the inverse problem by 1.5 times.

Some peculiar properties of the proposed method of imaging nanoparticles in biological tissues should be noted.

1. In this paper, the successful application of ANN for detection of nanoparticles in biological objects using the fluorescent signal (i.e., for the case of fluorescence spectroscopy, when only simple inexpensive equipment is required) was demonstrated. The elaborated method is fast, sensitive, inexpensive, and nondestructive. It has broad prospects in bionanomedicine.

2. An important advantage of using ANN is that the training of neural networks already takes all possible interactions of nanoparticles with biomacromolecules into account. Of course, each specific network is able to work with only the specified object. For another bio-object and other nanoparticles, new ANN training is required using appropriate experimental sets.

Acknowledgments

This work was supported in part by grant from Russian Academy of Science (RAS), Programme No. 24 (I.V.), by grant RFBR Russia-Egypt 15-52-61025 (I.V.), by Academy of Finland Project Nos. #137101, 260599, and 278812 (J.M.R.). The authors have no conflicts of interest to report. Authors are grateful to Gary McGuire for editing the manuscript.

References

1. M. H. Niemz, *Laser-Tissue Interactions: Fundamentals and Applications*, Springer, Berlin (1996).
2. R. Jianghong, A. Dragulescu-Andrasi, and Y. Hequan, "Fluorescence imaging in vivo: recent advances," *Curr. Opin. Biotechnol.* **18**, 17–25 (2007).
3. A. Vollrath, S. Schubert, and U. S. Schubert, "Fluorescence imaging of cancer tissue based on metal-free polymeric nanoparticles," *J. Mater. Chem. B* **1**, 1994–2007 (2013).
4. M. Zellweger, *Fluorescence Spectroscopy of Exogenous, Exogenously-Induced and Endogenous Fluorofores for the Photodetection and Photodynamic Therapy of Cancer*, Fevrier, Lausanne (2000).
5. D. Evanko, "The new fluorescent probes on the block," *Nat. Methods* **5**, 218–219 (2008).
6. A. P. Demchenko, *Introduction to Fluorescence Sensing*, Springer Science + Business Media B. V., The Netherlands (2009).
7. L. M. Wysocki and L. D. Lavis, "Advances in the chemistry of small molecule fluorescent probes," *Curr. Opin. Chem. Biol.* **15**(6), 752–759 (2011).
8. V. A. Oleinikov, A. V. Sukhanova, and I. R. Nabiev, "Fluorescent semiconductive nanocrystalls in biology and medicine," *Russ. Nanotechnol.* **2**(1–2), 160–173 (2007).
9. V. Biju et al., "Semiconductor quantum dots and metal nanoparticles: syntheses, optical properties, and biological applications," *Anal. Bioanal. Chem.* **391**, 2469–2495 (2008).
10. D. Ho, *Nanodiamonds, Applications in Biology and Nanoscale Medicine*, Springer, New York (2009).
11. Y. Y. Hui, C. L. Cheng, and C. H. Chang, "Nanodiamonds for optical bioimaging," *J. Phys. D. Appl. Phys.* **43**, 374021–374031 (2010).
12. A. M. Schrand, S. A. Ciftan Hens, and O. A. Shenderova, "Nanodiamond particles: properties and perspectives for bioapplications," *Crit. Rev. Solid State Mater. Sci.* **34**, 18–74 (2009).
13. A. M. Schrand et al., "Are diamond nanoparticles cytotoxic," *J. Phys. Chem. B* **111**, 2–7 (2007).
14. C. Fu et al., "Characterization and application of single fluorescent nanodiamonds as cellular biomarkers," *Proc. Natl. Acad. Sci. U. S. A.* **104**(3), 727–732 (2007).
15. T. A. Dolenko et al., "Study of adsorption properties of functionalized nanodiamonds in aqueous solutions of metal salts using optical spectroscopy," *J. Alloys Compd.* **586**, S436–S439 (2014).
16. T. A. Dolenko et al., "Diamond-water coupling effects in Raman and photoluminescence of nanodiamond colloidal suspensions," *J. Phys. Chem. C* **116**, 24314–24319 (2012).
17. S. C. Hens et al., "Photoluminescent nanostructures from graphite oxidation," *J. Phys. Chem. C* **116**, 20015–20022 (2012).
18. P. G. Luo et al., "Carbon "quantum" dots for optical bioimaging," *J. Mater. Chem. B* **1**, 2116–2127 (2013).
19. L. Cao et al., "Carbon dots for multiphoton bioimaging," *J. Am. Chem. Soc.* **129**, 11318–11319 (2007).
20. O. Shenderova et al., "Carbon dot: decorated nanodiamonds," *Part. Part. Syst. Char.* **31**(5), 580–590 (2014).
21. R. B. Gupta and U. B. Kompella, Eds., *Nanoparticle Technology for Drug Delivery*, Taylor & Francis Group LLC, New York (2006).
22. J. M. Rosenholm, C. Sahlgren, and M. Linden, "Towards multifunctional, targeted drug delivery systems using mesoporous silica nanoparticles: opportunities & challenges," *Nanoscale* **2**, 1870–1883 (2010).
23. L. Gu et al., "In vivo time-gated fluorescence imaging with biodegradable luminescent porous silicon nanoparticles," *Nat. Commun.* **4**, 2326–2332 (2013).
24. H. von E et al., "Core-shell designs of photoluminescent nanodiamonds with porous silica coatings for bioimaging and drug delivery I: fabrication," *J. Mater. Chem. B* **1**(18), 2358–2366 (2013).
25. N. Prabhakar et al., "Core-shell designs of photoluminescent nanodiamonds with porous silica coatings for bioimaging and drug delivery II: application," *Nanoscale* **5**(9), 3713–3722 (2013).
26. C. Cremer and T. Cremer, "Considerations on a laser-scanning microscope with high resolution and depth of field," *Microsc. Acta.* **81**(1), 31–44 (1978).
27. A. V. Feofanov, "Spectral laser scanning confocal microscopy in biological research," *Usp. Biol. Khim.* **47**, 371–410 (2007) (In Russian).
28. L. W. Zhang and N. A. Monteiro-Riviere, "Use of confocal microscopy for nanoparticle drug delivery through skin," *J. Biomed. Opt.* **18**(6), 061214 (2013).
29. S. Klein et al., "Quantification of colloidal and intracellular gold nanomarkers down to the single particle level using confocal microscopy," *Proc. SPIE* **7573**, 75730L (2010).
30. D. O. Lapotko, E. Y. Lukianova, and S. A. Chizhik, "Methods for monitoring and imaging nanoparticles in cells," *Proc. SPIE* **6447**, 644703 (2007).
31. X. Qu et al., "Imaging of cancer cells by multiphoton microscopy using gold nanoparticles and fluorescent dyes," *J. Biomed. Opt.* **13**(3), 031217 (2008).
32. S. Kantelhardt et al., "Multi-photon excitation fluorescence microscopy of brain-tumour tissue and analysis of cell density," *Acta Neurochir.* **151**, 253–262 (2009).
33. A. C. Curry, M. Crow, and A. Wax, "Molecular imaging of epidermal growth factor receptor in live cells with refractive index sensitivity using dark-field microspectroscopy and immunotargeted nanoparticles," *J. Biomed. Opt.* **13**(1), 014022 (2008).

34. F. Verpillat et al., "Dark-field digital holographic microscopy for 3-D-tracking of gold nanoparticles," *Opt. Express* **19**(27), 26044–26055 (2011).
35. T. Zhang et al., "Photoacoustic contrast imaging of biological tissues with nanodiamonds fabricated for high near-infrared absorbance," *J. Biomed. Opt.* **18**(2), 026018 (2013).
36. M. H. Xu and L. H. V. Wang, "Photoacoustic imaging in biomedicine," *Rev. Sci. Instrum.* **77**(4), 041101 (2006).
37. E. Garai et al., "High-sensitivity, real-time, ratiometric imaging of surface-enhanced Raman scattering nanoparticles with a clinically translatable Raman endoscope device," *J. Biomed. Opt.* **18**(9), 096008 (2013).
38. C. L. Zavaleta et al., "Preclinical evaluation of Raman nanoparticle biodistribution for their potential use in clinical endoscopy imaging," *Small* **7**(15), 2232–2240 (2011).
39. Z. Song et al., "Background free imaging of upconversion nanoparticle distribution in human skin," *J. Biomed. Opt.* **18**(6), 061215 (2013).
40. D. K. Chatterjee, M. K. Gnanasammandhan, and Y. Zhang, "Small upconverting fluorescent nanoparticles for biomedical applications," *Small* **6**(24), 2781–95 (2010).
41. E. A. Grebenik et al., "Feasibility study of the optical imaging of a breast cancer lesion labeled with upconversion nanoparticle biocomplexes," *J. Biomed. Opt.* **18**(7), 076004 (2013).
42. A. Dupont and D. C. Lamb, "Nanoscale three-dimensional single particle tracking," *Nanoscale* **3**(11), 4532–4541 (2011).
43. R. Igarashi et al., "Real-time background-free selective imaging of fluorescent nanodiamonds in vivo," *Nano Lett.* **12**, 5726–5732 (2012).
44. A. Hegyi and E. Yablonovitch, "Molecular imaging by optically-detected electron spin resonance of nitrogen-vacancies in nanodiamond," *Nano Lett.* **13**, 1173–1178 (2013).
45. S. K. Sarkar et al., "Wide-field in vivo background free imaging by selective magnetic modulation of nanodiamond fluorescence," *Biomed. Opt. Express* **5**, 1190–202 (2014).
46. M. H. Hassoun, *Fundamentals of Artificial Neural Networks*, MIT Press, Cambridge, Massachusetts (1995).
47. E. Keedwell, *Intelligent Bioinformatics: The Application of Artificial Intelligence Techniques to Bioinformatics Problems*, John Wiley & Sons Ltd., Chichester, England (2005).
48. I. V. Gerdova et al., "New opportunity solutions to inverse problems in laser spectroscopy involving artificial neural networks," *Izv. Akad. Nauk Ser. Fiz.* **66**(8), 1116–1124 (2002) (In Russian).
49. S. A. Dolenko et al., "Laser fluorimetry of mixtures of polyatomic organic compounds using artificial neural networks," *Quantum Electron.* **31**(9), 834–838 (2001).
50. S. A. Dolenko et al., "Adaptive methods for solving inverse problems in laser Raman spectroscopy of multi-component solutions," *Pattern Recognit. Image Anal.* **22**(4), 551–558 (2012).
51. A. Ya. Chervonenkis, "Application of methods of pattern recognition in the problems of molecular biology," *Probl. Upr.* **4**, 41–46 (2005) (In Russian).
52. T. Dramićanin et al., "Optical biopsy method for breast cancer diagnosis based on artificial neural network classification of fluorescence landscape data," *Acta Phys. Pol. A* **116**, 690–692 (2009).
53. L. Lenhardt et al., "Artificial neural networks for processing fluorescence spectroscopy data in skin cancer diagnostics," *Phys. Scr.* **T157**, 014057 (2013).
54. S. A. Burikov et al., "Use of neural network algorithms for elaboration of fluorescent biosensors on the base of nanoparticles," *Opt. Mem. Neural Netw. (Inform. Opt.)* **22**(3), 156–165 (2013).
55. S. Dolenko et al., "Comparison of input data compression methods in neural network solution of inverse problem in laser Raman spectroscopy of natural waters," *Lect. Notes Comput. Sci.* **7553**, 443–450 (2012).
56. Ward Systems Goup, Inc., "Advanced Neural Network and Genetic Algorithm Software, NeuroShell 2," 1997-2007, http://www.wardsystems.com/neuroshell2.asp (03 November 2014).

Tatiana A. Dolenko is a senior research scientist in M. V. Lomonosov Moscow State University (Physical Department), the Head of Laboratory of Laser Spectroscopy of Solutions of Supramolecular Compounds and Nanostructures. She received her PhD degree in physics in 1987. She is Laureate of Lenin Komsomol Prize in the field of Science and Technology (1985). She has authored about 130 papers. Her research interests include Raman and IR spectroscopy, aqueous solutions, nanostructures, suspensions of nanoparticles, and inverse problems.

Sergey A. Burikov is a senior research scientist at M.V. Lomonosov Moscow State University (Department of Physics). He received his PhD degree in physics and mathematics in 2008. He is the author of more than 40 papers. He is a repeated winner of Moscow State University Scholarship for talented young researchers and lecturers. His research includes Raman and IR spectroscopy, fluorimetry, aqueous solutions, and suspensions of nanoparticles.

Alexey M. Vervald entered the Physical Department of M.V.Lomonosov Moscow State University as a student in 2010. In 2012, he began his work on investigation of suspensions of nanodiamonds, with the purpose of their use as biomarkers in biomedicine. Since that time he works on the solution of inverse problems of laser spectroscopy via adaptive methods of data analysis and already has three publications.

Igor I. Vlasov received his MS degree in physics from the Physics Department of Moscow State University in 1983. He received his PhD degree in physics in 1993 for development of a new technique of atomic spectroscopy, laser enhanced ionization. In 1995, he joined the General Physics Institute, where his research interests focus on developing advanced carbon nanomaterials for photonics, quantum information processing, and biomedicine. Now he is head of the group for laser spectroscopy of carbon materials.

Sergey A. Dolenko received his candidate degree in physics and mathematics in 2002. He is a senior research scientist in D. V. Skobeltsyn Institute of Nuclear Physics, M. V. Lomonosov Moscow State University. He is the author of about 120 papers. He is a member of the Russian Neural Network Society and of the Russian Association of Pattern Recognition and Image Analysis. His research interests include artificial neural networks, genetic algorithms, adaptive methods of data analysis, inverse problems, spectroscopy.

Kirill A. Laptinskiy entered the Physical Department of M.V.Lomonosov Moscow State University as a student in 2008. In 2010, he began his work on investigation of suspensions of nanodiamonds, with the purpose of their use as biomarkers and adsorbents. At the beginning of 2014 he became a PhD student. His research interests include Raman and IR spectroscopy, fluorimetry, aqueous solutions, and suspensions of nanoparticles.

Jessica M. Rosenholm holds an adjunct professorship (title of docent) in biomedical nanotechnology at Åbo Akademi University, Finland. After a postdoctoral visit at Nano Biomedical Research Center, Shanghai Jiao Tong University in China, she heads the BioNanoMaterials Group (www.fyke.fi/bionano) at the Laboratory for Physical Chemistry at ÅAU. The group's activities are centered around the development of functional nanoparticles for detection, tracking, diagnostic and therapeutic biomedical applications, based largely on mesoporous silica and its composite nanostructures.

Olga A. Shenderova is the president of Adámas Nanotecnologies, USA. She received her PhD degree in materials science from St. Petersburg State Technical University, Russia. Her research interests include nanodiamond (ND) particle surface modification, production of fluorescent NDs, ND-based additives to lubricants, polymer composites, optical and biological applications of ND, and atomistic simulations of carbon nanostructures. She has authored over 140 papers, 15 book chapters, 20 patents, and edited 5 books related to nanodiamonds.